LumiNet: Perception-Driven Knowledge Distillation via Statistical Logit Calibration

Anonymous authors
Paper under double-blind review

Abstract

In knowledge distillation literature, feature-based methods have dominated due to their ability to effectively tap into extensive teacher models. In contrast, logit-based approaches, which aim to distill 'dark knowledge' from teachers, typically exhibit inferior performance compared to feature-based methods. To bridge this gap, we present LumiNet, a novel knowledge distillation algorithm designed to enhance logit-based distillation. We introduce the concept of 'perception', aiming to calibrate logits based on the model's representation capability. This concept addresses overconfidence issues in logit-based distillation method while also introducing a novel method to distill knowledge from the teacher. It reconstructs the logits of a sample/instances by considering relationships with other samples in the batch. LumiNet excels on benchmarks like CIFAR-100, ImageNet, and MSCOCO, outperforming leading feature-based methods, e.g., compared to KD with ResNet18 and MobileNetV2 on ImageNet, it shows improvements of 1.5% and 2.05%, respectively.

1 Introduction

The advancement in deep learning models has undergone significant increases in both complexity and performance. However, this progress brings challenges associated with computational demands and model scalability. To mitigate this, knowledge distillation (KD) has been proposed as an efficient strategy (Hinton et al., 2015) to transfer knowledge from a larger, intricate model (teacher) to a more compact, simpler model (student). The primary objective is to trade off performance and computational efficiency. There are two broad categories of KD: logit and feature-based strategies (Romero et al., 2014; Tian et al., 2020; Tung & Mori, 2019; Yim et al., 2017). The logit-based methods aim to match the output distributions of the teacher and student models (Zhang et al., 2018; Mirzadeh et al., 2020; Zhao et al., 2022). In contrast, feature-based methods are centered on aligning the intermediate layer representations between the two models (Romero et al., 2014). In general, it has been observed that feature-based KD outperforms logit-based KD (Zhao et al., 2022). However, feature-based KD suffers from layer misalignment (Romero et al., 2014) (reducing sample density in this space), privacy concerns (Goodfellow et al., 2015) (intermediate model layers accessible for adversarial attacks revealing training data and posing significant threats), and escalating computational requirements (Vaswani et al., 2017; Zhao et al., 2022) (see Fig. 1). These issues raise questions about its effectiveness, particularly in industrial applications. Similarly, these issues underscore the potential merits of logit-based KD over feature-based KD. This paper aims to enhance the effectiveness of logit-based knowledge distillation by leveraging its underlying strengths.

Several reasons underpin the disparity between logit- and feature-based KD. **Firstly**, one significant challenge in logit-based distillation, including data distillation(Zhu et al., 2023), is the issue of overconfidence. This is a common feature of any high-capacity pre-trained teacher model, which tends to assign the highest probability to the target class and shows a high variance in the probability distribution. The primary objective of traditional KD, particularly for the lower-capacity student model, is not just to match the target class probabilities but also to extract the 'dark knowledge' from the teacher model. The 'dark knowledge' refers to the knowledge encoded by the relative probabilities of the non-target classes (Yang et al., 2018; Furlanello et al., 2018; Hinton et al., 2015). However, a key issue is a substantial difference in confidence levels between target and non-target classes, as evidenced in Fig. 1. Even though temperature scaling (Hinton et al.,

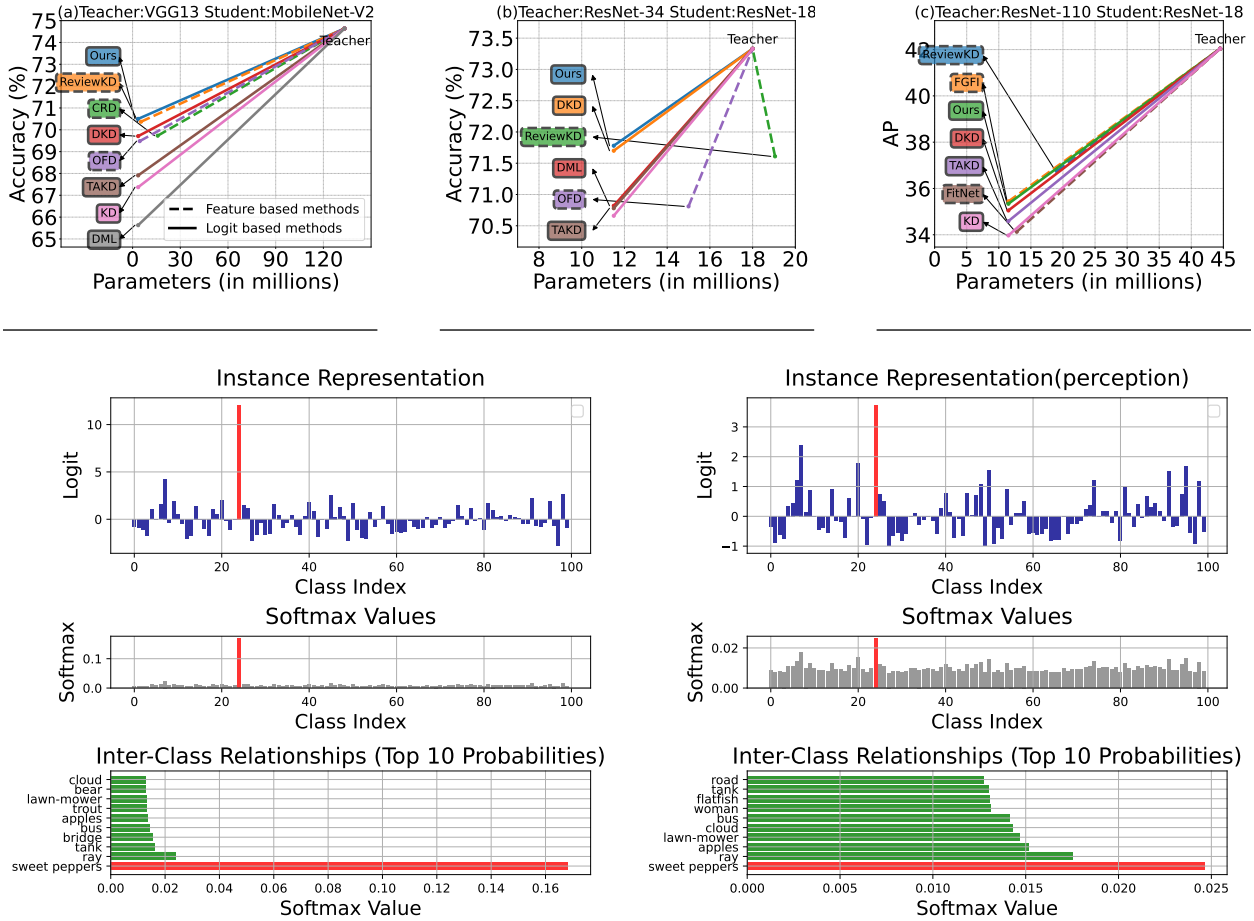

(d) CIFAR-100 - Before Perception

(e) CIFAR-100 - After Perception

Figure 1: Performance comparison of feature-based and logit-based methods on **(a)** CIFAR-100, **(b)** ImageNet, and **(c)** MS COCO datasets. Our proposed LumiNet, a logit-based method, achieves high accuracy without using extra parameters. **(d-e):** An example of ***(Left)*** before and ***(Right)*** after applying our proposed concept perception' on teacher's predicted probabilities. The first set of plots in the top row shows spikes in raw logits for the targeted class (Sweet Peppers, represented in red). This representation changes after the application of perception. Notably, various classes exhibit similar magnitudes to the targeted class, indicating reduced specificity. In the second set, despite conventional knowledge distillation softening, as seen in the left figure, there's persistent overconfidence in the target class. Perception minimizes the difference in softmax values between targeted and non-targeted classes, as depicted in the right figure. The third set illustrates inter-class relationships among the top 10 classes. While conventional scenarios (left) maintain these relationships, the perception method significantly alters them (right).

2015) is employed to address this, determining the optimal value to achieve proper alignment in learning remains an issue (Kim et al., 2021; Chen et al., 2021a; Wang & Yoon, 2021). Moreover, previous attempts to address the issue have led to increased complexity and computational load by introducing multiple objective functions(Zhao et al., 2022; Jin et al., 2023). **Secondly**, most of the logit-based methods often employ a simplistic matching criterion, which might not be robust enough to handle complex logit distributions for the student model, leading to suboptimal knowledge transfer (Romero et al., 2014; Chen et al., 2021a; Wang & Yoon, 2021). **Thirdly**, logit-based KD tends to struggle with granularity. Feature-based methods leverage a broader spectrum of the teacher's knowledge by aligning intermediate representations, providing richer information to the student (Heo et al., 2019a; Bengio et al., 2013; Wang & Yoon, 2021). In contrast, logits provide a more condensed representation, which might not always encapsulate the entirety of the teacher's knowledge (Romero et al., 2014). In addition, the student model learns the distribution of each instance independently in logit-based distillation without considering the distribution of other instances. This leads

to teacher-student fooling Ojha et al. (2023), where the student model may replicate errors or biases present in the teacher's logits for individual instances, affecting its overall performance and generalization. These inherent challenges associated with logit-based distillation necessitate the development of a novel method that strikes a balance between simplicity and effectiveness, mitigating overconfidence issues and enhancing sample representation for better knowledge extraction.

In response to the above challenges, we present LumiNet, a novel approach to knowledge distillation algorithms.The key focus of LumiNet is to generate a new representation of instance-level logit distributions. This representation is expected to effectively address all the issues of the knowledge distillation process discussed earlier. To enhance the model's representation, we focus on the statistical characteristics, mean and variance, of the model output. When focusing on a specific class, we analyze a vector field containing logit values for that class across various samples. Within this vector, we calculate deviation scores (original - mean) for logits, aiding in pinpointing anomalies and highest or lowest logit values. Additionally, by computing the variance, we gain insight into the interrelations among class values. Standardizing logits within the vector provides known statistics, ensuring that, for a particular class vector, the mean of logits is zero (with the maximum value receiving the highest positive score and the minimum value getting the least negative score). While these statistics hold consistently within isolated vector fields, applying this approach to all vector fields in the batch enables the formation of a novel inter-class relationship for each sample/instance. The resulting transformation produces a distinctive representation, which we term 'perception', for each sample, capturing essential insights from the collective statistical behaviors of individual class vectors. This approach effectively addresses overconfidence issues and capacity gaps, eliminating the dark knowledge concept, as illustrated in Fig. 1(d-e). By incorporating the internal relations of other samples/instances within the class, each logit value gains contextual insights, mitigating overconfidence and confirmation bias issues and facilitating the extraction of more subtle knowledge, as evidenced by improved performance scores.

Luminet draws inspiration from Kurt Lewin's Field Theory in Gestalt Psychology Lindorfer (2021), which emphasizes that perception is shaped by the overall psychological field or environment surrounding an entity. Lewin's concept suggests that human goals and behaviors are shaped or reshaped by psychological forces—positive forces drive us toward goals, while negative forces push us away from undesired outcomes. Just as humans perceive objects, Luminet adapts this principle to machine learning. Lumnet dynamically adjusts each sample's representation by leveraging interactions within the surrounding field (the field here is the entire batch), where the forces exerted by other samples influence these adjustments. If a sample encounters suboptimal conditions (overconfidence, errors), the representations of neighboring samples collaborate to minimize its degradation, enhancing overall model robustness. The name "perception" reflects this core idea from Kurt Lewin's Field Theory in Gestalt Psychology.

The performance of LumiNet is evaluated on three computer vision tasks: image recognition, object detection, and transfer learning for feature transfer ability. Our empirical evaluations solidify the efficacy of LumiNet: for instance, using ResNet8x4 as a student, we achieved a notable 77. 5% precision and further established benchmark supremacy across tasks on datasets such as CIFAR100, ImageNet, MS-COCO, and TinyImageNet.

Our contributions are as follows:

- We introduce LumiNet, a novel knowledge distillation algorithm that replaces the traditional dark knowledge concept. It addresses issues of overconfidence, capacity gaps, and teacher-student fooling, while incorporating contextual knowledge into logits by creating new representations for samples.

- Through extensive empirical evaluations, we demonstrate that our method consistently enhances performance across diverse datasets (CIFAR100, ImageNet, MS-COCO, and TinyImageNe), deep learning architectures (ResNet, VGG, ShuffleNet, MobileNet, WRN, and Faster-RCNN-FPN), and tasks (recognition, detection, and transfer learning).

2 Related Works

Logit-based KD: In the domain of KD, logit-based techniques have traditionally emphasized the distillation process utilizing solely the output logits. Historically, the primary focus of research within logit distillation has been developing and refining regularization and optimization strategies rather than exploring novel methodologies. Noteworthy extensions to this conventional framework include the mutual-learning paradigm, frequently referenced as DML (Zhang et al., 2018), and incorporating the teacher assistant module, colloquially termed TAKD (Mirzadeh et al., 2020). Nonetheless, a considerable portion of the existing methodologies remain anchored to the foundational principles of the classical KD paradigm, seldom probing the intricate behaviors and subtleties associated with logits (Zhao et al., 2022). A novel approach to object detection distillation, combining feature-based and logit-based methods with a closed-loop knowledge distillation framework, has demonstrated improved accuracy and robustness compared to existing state-of-the-art techniques (Song et al., 2024). While the versatility of these logit-based methods facilitates their applicability across diverse scenarios, empirical observations suggest that their efficacy often falls short when juxtaposed against feature-level distillation techniques.

Feature-based KD: Feature distillation, a knowledge transfer strategy, focuses on utilizing intermediate features to relay knowledge from a teacher model to a student model. State-of-the-art methods have commonly employed this technique, with some working to minimize the divergence between features of the teacher and student models (Heo et al., 2019b;a; Romero et al., 2014). A richer knowledge transfer is facilitated by forcing the student to mimic the teacher at the feature level. Others have extended this approach by distilling input correlations, further enhancing the depth of knowledge transfer (Park et al., 2019; Tian et al., 2020; Tung & Mori, 2019; Chen et al., 2021b). DiffKD (Huang et al., 2024), a novel knowledge distillation method utilizing diffusion models to denoise and align student features with teacher features, has demonstrated state-of-the-art performance across image classification, object detection, and semantic segmentation tasks These methods, though high-performing, struggle with substantial computational demands and potential privacy issues, especially with complex models and large datasets. These challenges not only amplify processing time and costs but can also limit their practical applicability in real-world scenarios. Recognizing these challenges, we turn our attention to logit-based distillation techniques.

Applications with KD: Rooted in foundational work by (Hinton et al., 2015) and further enriched by advanced strategies like Attention Transfer (Zagoruyko & Komodakis, 2017), ReviewKd (Chen et al., 2021b), Decoupled KD (Zhao et al., 2022) and other methods (Park et al., 2019; Tian et al., 2020), KD has significantly improved performance in core vision tasks, spanning recognition (Krizhevsky et al., 2012; Simonyan & Zisserman, 2014; He et al., 2016), segmentation(Qin et al., 2021; Liu et al., 2019), and detection (Li et al., 2022a; Yang et al., 2022; Zheng et al., 2023; Xu et al., 2022). Beyond vision, KD has also made notable strides in NLP tasks like machine translation and sentiment analysis (Kim & Rush, 2016; Zhang et al., 2022). KD has proven valuable in addressing broader AI challenges, such as reducing model biases (Hossain et al., 2022; Chai et al., 2022; Zhou et al., 2021; Jung et al., 2021) and strengthening common-sense reasoning (West et al., 2022). We evaluate our method within the realms of image classification and object detection.

3 Methodology

3.1 Knowledge Distillation Revisited

Consider a set of distinct samples denoted $\mathcal{X} = \{\mathbf{x}_i\}_{i=1}^{n}$, where $\mathbf{x}_i \in \mathbb{R}^m$ and n represent the total number of samples. Given a parametric deep learning model f_θ with learnable parameters θ, its output for a sample $\mathbf{x}_i$ is defined as $\mathbf{z}_i = f(\mathbf{x}_i)$, where $\mathbf{z}_i \in \mathbb{R}^c$, and c denotes the number of classes within the sample set $\mathcal{X}$. In the context of KD literature, the model's output $\mathbf{z}$ is often referred to as the logit of the model. For brevity, we will omit θ from the model notation f. To provide more context within the realm of knowledge distillation, we designate f_T as the teacher model and f_S as the student model. The fundamental objective of KD is to minimize the divergence between the logits of the student and teacher for each sample in $\mathcal{X}$. This can be expressed mathematically as minimizing the objective,$L_{\text{KD}} = \sum_{\mathbf{x}_i \in \mathcal{X}} \ell\left(f_T(\mathbf{x}_i), f_S(\mathbf{x}_i)\right)$. Here, $\ell(\cdot, \cdot)$ is a loss function that measures the discrepancy between two vectors. For logit-based distillation, the primary objective is to align the softened logits of the student and teacher models. This alignment is quantified using

the Kullback-Leibler (KL) divergence between the softened probabilities of the two models. Formally, the distillation loss, L_{KD}, is defined as:

$$L_{KD} = KL\left(\text{Softmax}\left(\frac{f_T(\mathbf{x}_i)}{\tau}\right) \,||\, \text{Softmax}\left(\frac{f_S(\mathbf{x}_i)}{\tau}\right)\right) \tag{1}$$

Here, τ is the temperature parameter that modulates the softmax sharpness.

The primary hurdles with logit-based distillation lie in the fact that any logit vector $\mathbf{z}_i = f(\mathbf{x}_i)$ is considerably more compact than its feature vector counterpart. Another challenge is the tendency for overconfidence, especially when the output $\mathbf{z}_i$ is from a pre-trained teacher model. Overly confident teacher predictions in knowledge distillation pose a critical issue where $P(y = t|x) \to 1$ for target class t, consequently forcing $P(y = i|x) \to 0$ for all non-target classes i. This extreme probability distribution effectively suppresses the valuable "dark knowledge" encoded in the relative magnitudes of non-target class probabilities, which Hinton et al. (2015) identified as crucial information for student learning. The resulting near-zero probabilities cause gradient signal degradation during KL-divergence minimization, making it challenging for the student to capture the subtle inter-class relationships that contribute to the teacher's generalization capabilities. These aspects make it difficult for the student model to extract the full range of knowledge embedded in the teacher model (Romero et al., 2014). The following section outlines some potential limitations associated with logit-based knowledge distillation.

(1) Efficiency and Knowledge Representation: In neural networks, decision-making frequently relies on the probabilities assigned to specific classes for individual instances or samples (Yegnanarayana, 2009). For example, if the probability of an instance x_i belonging to class c_1 is close to the probability of it belonging to class c_2, we infer that the two classes are likely to represent similar objects or share common features. We heavily rely on this representation in knowledge distillation, and the student model aims to grasp this pattern (Zhao et al., 2022; Zhang et al., 2018; Mirzadeh et al., 2020). To achieve this, leading logit-based distillation methods often employ multiple objective functions to capture essential information (Zhao et al., 2022; Jin et al., 2023). For instance, Decouple Knowledge Distillation (DKD) (Zhao et al., 2022) uses two objective functions to understand the patterns of target and non-targeted classes separately. However, this approach increases the number of hyperparameters and may pose challenges for industrial applications. On the other hand, MLLD (Jin et al., 2023) adopts multi-level distillation, involving multiple objective functions and introducing computational complexities along with additional hyperparameters. This complexity gives rise to considerations about the feasibility of applying these methods to extensive tasks and industrial contexts. The fundamental question arises: Can we formulate a novel instance representation that simplifies instance-level distillation, mirroring the simplicity of traditional KD? If attainable, this prospect could open the door for a new research trajectory in knowledge distillation, as there would be no need to directly extract relative information about classes from the teacher, which is the core philosophy of KD.

(2) Role of τ: In knowledge distillation, the temperature scaling softens the outputs of the teacher's model, serving as a regularizer to reduce overfitting. Moreover, by preventing premature over-confidence in predictions, τ further promotes better generalization and reduces the risk of fitting too closely to training data (Hinton et al., 2015). Because the outputs of the teacher and student model have inherent statistical differences, finding a suitable value for τ is difficult (Liu et al., 2023b). Usually, KD methods require extensive τ fine-tuning, leading to additional computational costs (Rafat et al., 2023).

3.2 Introducing LumiNet

Based on our previous discussion, the process of knowledge distillation is found to be further enriched for a given instance $\mathbf{x}_i$ when viewed in the context of its batch samples. The overconfidence issues in inter-class relationships inside instances are also mitigated.

Formally, a measure of information K corresponding to $\mathbf{x}_i$ can be obtained as:

$$K(\mathbf{x}_i) \propto \mathcal{D}(\mathbf{x}_i) + \sum_{j \neq i} R(\mathbf{x}_i, \mathbf{x}_j) \tag{2}$$

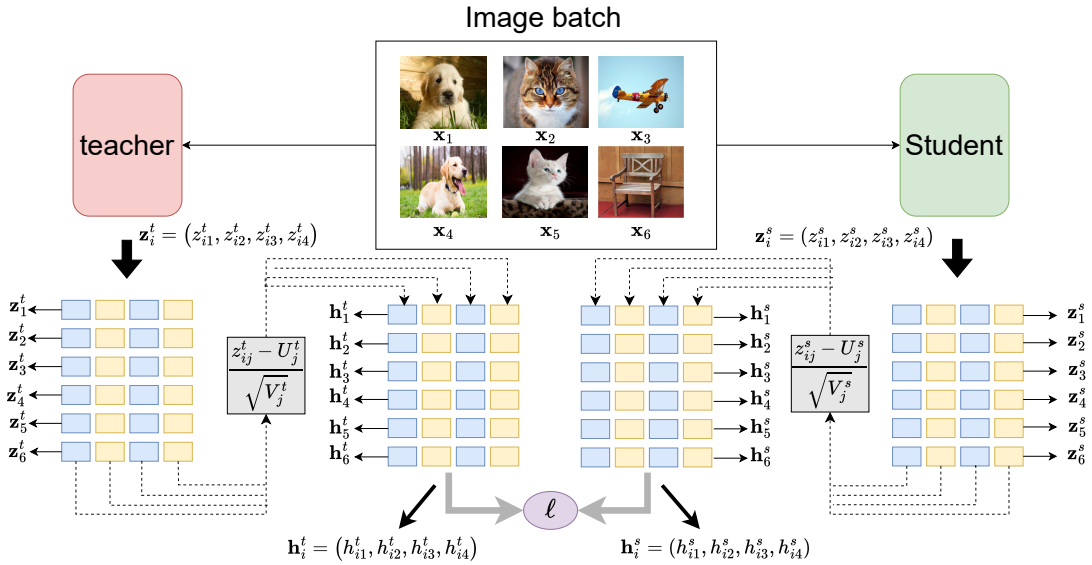

Figure 2: Given a batch of samples $\mathcal{B} = \{\mathbf{x}_1, \mathbf{x}_2, \mathbf{x}_3, \mathbf{x}_4, \mathbf{x}_5, \mathbf{x}_6\}$, both the teacher and student models generate logit for each sample in the batch, denoted as $\mathbf{z}_i^t = (z_{i1}^t, z_{i2}^t, z_{i3}^t, z_{i4}^t)$ and $\mathbf{z}_i^s = (z_{i1}^s, z_{i2}^s, z_{i3}^s, z_{i4}^s)$. In the subsequent stage, $mean((U_j^t, U_j^s))$ and $variance(V_j^t, V_j^s)$ for each class in the batch are computed for both teacher and student logit. These values are then used to normalize the logit of both models, resulting in a new logit representation referred to as the Perception logit: $\mathbf{h}_i^t = (h_{i1}^t, h_{i2}^t, h_{i3}^t, h_{i4}^t)$ and $\mathbf{h}_i^s = (h_{i1}^s, h_{i2}^s, h_{i3}^s, h_{i4}^s)$. Finally, a loss function ℓ is calculated between the teacher and student to complete the knowledge distillation process.

Let $K(\mathbf{x}_i)$ be defined as an information measure that quantifies the total information content of an instance $\mathbf{x}_i$. $\mathcal{D}(\mathbf{x}_i)$ refers to the intra-class divergence measure, for instance $\mathbf{x}_i$, capturing how the instance relates to its assigned class and $R(\mathbf{x}_i, \mathbf{x}_j)$ means relational measure between instances $\mathbf{x}_i$ and $\mathbf{x}_j$, quantifying their mutual information in feature space.

Constructing the perception: We formulate our approach considering a batch of data samples $\mathcal{B} = \{\mathbf{x}_i\}_{i=1}^b$, which is randomly selected from the original dataset $\mathcal{X}$. Consequently, the logits generated by a model f for an instance $\mathbf{x}_i \in \mathcal{B}$ across c classes are represented as: $\mathbf{z}_i = (z_{i1}, z_{i2}, \ldots, z_{ic})$, where z_{ik} symbolizes the logit for the jth class for instance x_i. We adjust the logits based on the mean U_j and variance V_j across each class j of a batch. This transformed logit is given by:

$h_{ij} = \frac{z_{ij} - U_j}{\sqrt{V_j}}$. Here, h_{ij} represents the augmented logit for the jth class for instance $\mathbf{x}_i$. Consequently, the augmented logits for instance, $\mathbf{x}_i$ are obtained as:

$$\mathbf{h}_i = \left(\frac{z_{i1} - U_1}{\sqrt{V_1}}, \frac{z_{i2} - U_2}{\sqrt{V_2}}, \ldots, \frac{z_{ic} - U_c}{\sqrt{V_c}} \right) \tag{3}$$

In this context, the reconstructed logits $\mathbf{h}_i$ capture the model's perception. Instead of merely making raw predictions, both the models (teacher and student) try to understand the finer details and differences within the batch of data. As outlined in Eq. 3, the method of constructing 'perceived' logits is explained. In short, when both the teacher and student models' intra-class predictions are adjusted on the same scale, the probability distribution across all the classes for individual instances is influenced. This new set of logits offers us a more insightful representation of each instance. We refer to this set of logits $\mathbf{h}_i$ as 'perception'.

The LumiNet Loss: Classical knowledge distillation seeks to transfer the rich perceptual capabilities of a teacher model onto a smaller student model. To this end, we introduce LumiNet, a novel approach emphasizing the alignment of 'perceptions' rather than raw logits. In LumiNet, we focus on the perceived logits. Given an instance $\mathbf{x}_i$, we denote the logits from the teacher for class c as h_{ic}^t and those from the

	Teacher	KD	KD*	Ours
Temp	-	4	2	**4**
Entropy	0.03	0.42	0.40	**1.26**
Instance Variance	4.4	2.3	-	**0.91**
Mutual Information	3.64	3.60	3.56	**3.65**
Avg. Gradient L2 Norm	-	1.28	1.10	**3.27**
Gradient Variance	-	0.013	0.013	**0.015**
Accuracy	79.42	73.08	72.91	**77.50**

Table 1: Entropy Analysis

Model	FPR95 ↓	ECE ↓	MCE ↓
	CIFAR-100		
	CE / KD / Ours		
ResNet8×4	3.58 / 4.15 / **2.74**	0.09 / 0.11 / **0.06**	0.21 / 0.23 / **0.18**
VGG8	5.61 / 5.75 / **4.20**	0.13 / 0.12 / **0.06**	0.28 / 0.30 / **0.20**
MobileNet-V2	10.7 / 11.71 / **6.14**	0.17 / 0.21 / **0.09**	0.38 / 0.35 / **0.21**
WRN-40-1	4.13/4.59 / **3.51**	0.09 / 0.15 / **0.07**	0.17 / 0.34 / **0.14**

Table 2: Calibration Analysis

student as h^s_{ic}. The softmax operation scaled by a temperature factor τ produces probability distributions as: $P^T_c(\mathbf{x}_i) = \frac{\exp(h^t_{ic}/\tau)}{\sum_{c'} \exp(h^t_{ic'}/\tau)}$, $\quad P^S_c(\mathbf{x}_i) = \frac{\exp(h^s_{ic}/\tau)}{\sum_{c'} \exp(h^s_{ic'}/\tau)}$.

Thus, the LumiNet loss can be represented as:

$$\mathcal{L}_{LumiNet} = \sum_{\mathbf{x}_i \in \mathbf{X}} \sum_c P^T_c(\mathbf{x}_i) \log \frac{P^T_c(\mathbf{x}_i)}{P^S_c(\mathbf{x}_i)}, \tag{4}$$

The objective of the LumiNet loss (Eq. 4) is for the student model to align its 'perception' with the teacher, excluding the direct logit or inter-class relationships. This ensures that the student does not merely imitate the teacher's outputs but learns a deeper understanding of intra-class and inter-class relationships with a new representation (it also aligns with our intent outlined in Eq. 2). By minimizing the LumiNet loss, we ensure that the student model's perception or representation of instances closely mirrors the teacher's, leading to a more robust student model.

Total Loss Formulation: The complete training objective for our knowledge distillation framework combines the traditional cross-entropy loss $\mathcal{L}_{CE}$ with our proposed LumiNet loss $\mathcal{L}_{LumiNet}$. While $\mathcal{L}_{CE}$ operates on the raw logits $\mathbf{z}_i$ and ground truth labels y_i to ensure correct classification:

$$\mathcal{L}_{CE} = -\frac{1}{N} \sum_{i=1}^{N} \sum_{c=1}^{C} y_{ic} \log(\hat{y}_{ic}) \tag{5}$$

where $(\hat{y}_{ic})$ is the softmax probability, (y_{ic}) is the ground truth label, (N) is the batch size, and (C) is the number of classes. The $\mathcal{L}_{LumiNet}$ term works with the perceived logits $\mathbf{h}_i$ to transfer the teacher's perceptual knowledge to the student. The total loss is thus formulated as:

$$\mathcal{L}_{total} = \mathcal{L}_{CE} + \lambda \mathcal{L}_{LumiNet} \tag{6}$$

where λ is a balancing scalar that controls the contribution of the LumiNet loss. This dual-objective optimization ensures that the student model not only learns to correctly classify instances through $\mathcal{L}_{CE}$ but also acquires the teacher's rich perceptual understanding through $\mathcal{L}_{LumiNet}$.

3.3 Theoretical Foundations and Empirical Validation of LumiNet

(a) Information-Theoretic Perspective: The transformation of perception logit, shown in Eq. 3, can be analyzed using mutual information. Let Z be the random variable representing raw logits and H be the perception logits of the same sample. We can show that: $I(H;Y) \geq I(Z;Y)$ where Y is the true class label, and $I(H;Y)$ or $I(Z;Y)$ is mutual information. This inequality holds because the normalization process reduces noise and emphasizes class-relevant information. Our calculations show that our model surpassed the teacher's mutual information score of 3.65.

(b) Gradient Flow Enhancement: The gradient of the LumiNet loss (Eq. 4) with respect to the parameters of the student model θ_s can be expressed as: $\frac{\partial \mathcal{L}LumiNet}{\partial \theta_s} = \frac{\partial \mathcal{L}LumiNet}{\partial h_s} \cdot \frac{\partial h_s}{\partial z_s} \cdot \frac{\partial z_s}{\partial \theta_s}$ The term $\frac{\partial h_s}{\partial z_s} = \frac{1}{\sqrt{V_j}}$ acts as an adaptive learning rate, providing larger updates for classes with lower variance. This theoretically leads to more balanced learning across classes. We tracked the L2 norm of gradients during training for both traditional KD and LumiNet. LumiNet demonstrates a substantially higher average gradient L2 norm

(3.27) compared to KD (1.28) and KD* (1.10), indicating stronger parameter updates during training. The gradient 0variance for LumiNet (0.015) is slightly higher than KD and KD *, (also demonstrated in the convergence analysis Fig. 7), suggesting a more dynamic learning process while maintaining overall stability.

(c) Entropy Analysis: We measured the entropy of probability distributions derived from raw logits and perception logits across various datasets. The results consistently showed higher entropy for perception logits, as shown in Table 1. This increase in entropy suggests that the perception logits contain more information, supporting our claim in the theoretical analysis. The entropy of LumiNet, which is 1.26, is significantly higher than that of traditional KD (0.42), indicating a higher representation of logits.

(d) Calibration Analysis: To evaluate model calibration, we rely on three widely accepted metrics—FPR95, Expected Calibration Error (ECE) , and Maximum Calibration Error (MCE). These metrics comprehensively assess alignment between model confidence and accuracy, highlighting reliability (FPR95), overall calibration (ECE), and worst-case miscalibration scenarios (MCE). We understand overconfidence mitigation by observing improvements in metrics like FPR95, ECE, and MCE, where a lower value indicates fewer false high-confidence predictions and less extreme miscalibration, respectively. These metrics provide a robust framework for analyzing both overconfidence and calibration performance. Our experiments show that our method consistently outperforms models trained using traditional approaches, such as KD or Cross-Entropy (CE) loss, across all three metrics listed in (2). This outcome demonstrates our method's ability to improve calibration while reducing overconfidence in the model's predictions. Additionally, a discussion on the analysis of confirmation bias is included in the Appendix(A6).

3.4 The bright side of LumiNet perception

While conventional Knowledge Distillation frameworks face challenges in both logit-based and feature-based implementations, our proposed method sheds light on a renewed perspective to tackle these issues. Here is a detailed exploration of the bright side of LumiNet's approach to KD:

1. **Enhanced logit granularity with perception:** Traditional logit-based approaches are restricted by the inherent granularity of their representations, as characterized by the direct logits of any input $\mathbf{x}_i$. In contrast, LumiNet, leveraging its perception, refines this representation by introducing a transformation. Using the mean U_j and the variance V_j for the logarithms of each class within a batch, as defined in the perceived logits $\mathbf{h}_i$ in Eq. 3, LumiNet achieves a more nuanced understanding. This mathematical recalibration allows the model to encapsulate subtler distinctions and depth, addressing the limitations inherent to conventional logit presentations.

2. **Balanced softening and overfitting:** In traditional KD, the temperature parameter τ tempers logits by pushing their values closer to zero, effectively reducing variance and bridging the gap between teacher and student logits for efficient knowledge transfer. In LumiNet, logits $\mathbf{x}'_i$ are intra-class normalized, yielding a zero mean and unit variance for each class. Thus, the reliance on τ for inter-class adjustments is diminished due to the intrinsically reduced variance and mean of the logits.

In essence, LumiNet not only rectifies recognized challenges, but also paves the way to potentially enhance logit-based KD techniques to overshadow their feature-based counterparts.

4 Experiments

4.1 Setup

Dataset: Using benchmark datasets, we conducted experiments on three vision tasks: image classification, object detection, and transfer learning. Our experiments leveraged *four* widely acknowledged benchmark datasets. First, **CIFAR-100** (Krizhevsky et al., 2009), encapsulating a compact yet comprehensive representation of images, comprises 60,000 32x32 resolution images, segregated into 100 classes with 600 images per class. **ImageNet** (Russakovsky et al., 2015), a more extensive dataset, provides a rigorous testing ground

Table 3: Recognition results on the CIFAR-100 validation.

(a) Same architecture

Teacher	ResNet56	ResNet110	ResNet32×4	WRN-40-2	WRN-40-2	VGG13
	72.34	74.31	79.42	75.61	75.61	74.64
Student	ResNet20	ResNet32	ResNet8×4	WRN-16-2	WRN-40-1	VGG8
	69.06	71.14	72.50	73.26	71.98	70.36
Feature-Based Methods						
FitNet (Romero et al., 2014)	69.21	71.06	73.50	73.58	72.24	71.02
RKD (Park et al., 2019)	69.61	71.82	71.90	73.35	72.22	71.48
CRD (Tian et al., 2020)	71.16	73.48	75.51	75.48	74.14	73.94
OFD (Heo et al., 2019a)	70.98	73.23	74.95	75.24	74.33	73.95
ReviewKD (Chen et al., 2021b)	71.89	73.89	75.63	76.12	75.09	74.84
FCFD(Liu et al., 2023a)	71.68	-	76.80	76.34	75.43	74.86
Logit-Based Methods						
KD(Hinton et al., 2015)	70.66	73.08	73.33	74.92	73.54	72.98
DML(Zhang et al., 2018)	69.52	72.03	72.12	73.58	72.68	71.79
TAKD(Mirzadeh et al., 2020)	70.83	73.37	73.81	75.12	73.78	73.23
DKD(Zhao et al., 2022)	71.97	74.11	76.32	76.24	74.81	74.68
Ours	**72.29**	**74.2**	**77.50**	**76.38**	**75.12**	**74.94**
	(0.11)	(0.23)	(0.19)	(0.32)	(0.13)	(0.16)
Δ	+1.63	+1.12	+4.17	+1.37	+1.58	+1.96

(b) Different architecture

Teacher	ResNet32×4	WRN-40-2	VGG13	ResNet50	ResNet32×4
	79.42	75.61	74.64	79.34	79.42
Student	ShuffleNet-V1	ShuffleNet-V1	MobileNet-V2	MobileNet-V2	ShuffleNet-V2
	70.50	70.50	64.60	64.60	71.82
Feature-Based Methods					
FitNet (Romero et al., 2014)	73.59	73.73	64.14	63.16	73.54
RKD (Park et al., 2019)	72.28	72.21	64.52	64.43	73.21
CRD (Tian et al., 2020)	75.11	76.05	69.73	69.11	75.65
OFD (Heo et al., 2019a)	75.98	75.85	69.48	69.04	76.82
ReviewKD (Chen et al., 2021b)	77.45	77.14	70.37	69.89	77.78
FCFD(Liu et al., 2023a)	78.12	77.81	70.67	71.07	78.20
Logit-Based Methods					
KD(Hinton et al., 2015)	74.07	74.83	67.37	67.35	74.45
DML(Zhang et al., 2018)	72.89	72.76	65.63	65.71	73.45
TAKD(Mirzadeh et al., 2020)	74.53	75.34	67.91	68.02	74.82
DKD(Zhao et al., 2022)	76.45	76.70	69.71	70.35	77.07
Ours	**76.66**	**76.95**	**70.50**	**70.97**	**77.55**
	(0.08)	(0.15)	(0.10)	(0.12)	(0.21)
Δ	+2.59	+2.12	+3.13	+3.62	+3.1

with its collection of over a million images distributed across 1,000 diverse classes, often utilized to probe models for robustness and generalization. Concurrently, the **MS COCO** dataset (Lin et al., 2014), renowned for its rich annotations, is pivotal for intricate tasks, facilitating both object detection and segmentation assessments with 330K images, 1.5 million object instances, and 80 object categories. We strictly adhered to standard dataset splits for reproducibility and benchmarking compatibility for training, validation, and testing. The **TinyImageNet**[1] dataset, although more compact, acts as an invaluable resource for transfer learning experiments due to its wide variety across its 200 classes.

Network architectures: Various architectures are employed depending on the context. For CIFAR-100, homogeneous configurations use teacher models such as ResNet56, ResNet110 (He et al., 2016), and WRN-40-2, paired with corresponding students such as ResNet20 and WRN-16-2 (Table 3a). In heterogeneous settings, architectures such as ResNet32×4 and VGG13 (Simonyan & Zisserman, 2014) for teachers are paired with lightweight models like ShuffleNet-V1, ShuffleNet-V2 (Ma et al., 2018) and MobileNet-V2 (Sandler et al., 2018) as students (Table 3b). For ImageNet classification, ResNet34 was employed as the teacher and ResNet18 as the student. Additionally, for object detection on MS-COCO, Faster RCNN with FPN (Zhang et al., 2022) was utilized as a feature extractor, with predominant teacher models being ResNet variants, while the latter served as a student. A pre-trained WRN_16_2 model is further harnessed for transfer learning. We also performed tests on ViT models (Dosovitskiy et al., 2021). DeiT-Ti (Touvron et al., 2021), PiT-Ti(Heo et al., 2021), PVT-Ti(Wang et al., 2021), and PVTv2-B0(Wang et al., 2022) served as student models, with ResNet50 acting as the teacher model.

Evaluation metric: We assess methods' performance using Top-1 and Top-5 accuracy for classification tasks. We employ Average Precision (AP, AP50, and AP70) to gauge precision levels in object detection tasks. We calculate a Δ that denotes the performance improvement of LumiNet over the classical KD method, underlining the enhancements of our approach.

Implementation details: We explore knowledge distillation using two configurations: a homogeneous architecture, where both teacher and student models have identical architectural types (ResNet56 and

[1] https://www.kaggle.com/c/tiny-imagenet

Table 4: Reported are the Top-1 and Top-5 accuracy (%) on ImageNet validation.

			Feature-Based Methods				Logit-Based Methods					
ResNet34 (Teacher) and ResNet18 (Student)												
	Teacher	Student	AT	OFD	CRD	ReviewKD	KD	DML	TAKD	DKD	**Ours**	Δ
Top-1	73.31	69.75	70.69	70.69	70.81	71.17	70.66	70.82	70.78	71.70	**72.16**	+1.5
Top-5	91.42	89.07	90.01	90.01	89.98	90.13	89.88	90.02	90.16	90.41	**90.60**	+0.72
ResNet50 (Teacher) and MobileNet-V2 (Student)												
Top-1	76.16	68.87	69.56	71.25	71.37	72.56	70.50	71.35	70.82	72.05	**72.55**	+2.05
Top-5	92.86	88.76	89.33	90.34	90.41	91.00	89.80	90.31	90.01	91.05	**91.12**	+1.32

Table 5: Detection results on MS-COCO using Faster-RCNN-FPN (Lin et al., 2017) backbone.

			Feature-Based Methods			Logit-Based Methods				
ResNet101 (Teacher) and ResNet18 (Student)										
	Teacher	Student	FitNet	FGFI	ReviewKD	KD	TAKD	DKD	Ours	Δ
AP	42.04	33.26	34.13	35.44	**36.75**	33.97	34.59	35.05	35.34	+1.37
AP_{50}	62.48	53.61	54.16	55.51	56.72	54.66	55.35	56.60	**56.82**	+2.16
AP_{75}	45.88	35.26	36.71	**38.17**	34.00	36.62	37.12	37.54	37.56	+0.94
ResNet50 (Teacher) and MobileNet-V2 (Student)										
AP	40.22	29.47	30.20	31.16	**33.71**	30.13	31.26	32.34	32.38	+2.25
AP_{50}	61.02	48.87	49.80	50.68	53.15	50.28	51.03	53.77	**53.84**	+3.56
AP_{75}	45.88	30.90	31.69	32.92	36.13	31.35	33.46	34.01	33.57	+2.22

ResNet20), and a heterogeneous architecture, where they differ (ResNet32x4 as the teacher and ShuffleNet-V1 as the student). Our study incorporates a range of neural network architectures such as ResNet, WRN, VGG, ShuffleNet-V1/V2, and MobileNetV2. The training parameters are set as follows: for CIFAR-100, a batch size of 64 and a learning rate of 0.05; for ImageNet, a batch size of 128 and a learning rate of 0.1; and for MS-COCO, a batch size of 8 with a learning rate of 0.01. We followed the implementation settings of (Zhao et al., 2022). To implement distillation in the ViT variant, we adopted the implementation settings detailed by (Li et al., 2022b). All models are trained on a single GPU. Detailed implementation for each task can be found in the appendix.

4.2 Main Results

Comparison methods: We compare our method with well-established feature- and logit-based distillation methods, underscoring its potential and advantages in the knowledge distillation domain. Notable methods in *Feature Based Methods* category include FitNet (Romero et al., 2014), which aligns features at certain intermediary layers, RKD (Park et al., 2019) that focuses on preserving pairwise relations of examples, and CRD (Tian et al., 2020), which minimizes the contrastive loss between the representations of the teacher and student models. Other methods in this category include OFD (Cho & Hariharan, 2019) and ReviewKD (Chen et al., 2021b), each bringing unique strategies to leverage intermediary network features. *Logit Based Methods* methods include KD (Hinton et al., 2015), DML (Zhang et al., 2018), TAKD (Mirzadeh et al., 2020), and DKD (Zhao et al., 2022), which ensure that the student's logits are similar to the teacher's.

Recognition tasks: We perform image recognition tasks on CIFAR-100 and ImageNet. On **CIFAR-100**, when teacher and student models shared identical architectures, shown in Table 3a, LumiNet presented improvements of 2-3%. And when the architectures were from different series, shown in Table 3b, the improvements were between 3-4%, consistently outperforming the baseline, classical KD, and other methods rooted in KD's principles. Similarly, on the intricate **ImageNet** dataset, LumiNet outshined all logit-based distillation techniques and beat state-of-the-art feature-based distillation methods, shown in Table 4. These results consistently demonstrate that, regardless of variations in the dataset or architectural differences, LumiNet performs exceptionally well. In particular, it highlights the distinctive ability of LumiNet to learn based on the concept of 'perception.

In Table 6, we show that LumiNet demonstrates a superior trade-off between the number of extra parameters/running time vs. precision. The necessity for extra parameters in feature-based techniques arises from

Table 6: Comparison of training time per batch, number of extra parameters (θ) on the CIFAR-100.

Teacher: ResNet32×4 Student: ResNet8×4	KD	RKD	FitNet	OFD	CRD	ReviewKd	DkD	**Ours**
Latency↓ (ms)	11	25	14	19	41	26	11	**11**
$\theta \downarrow$	0	0	16.8K	86.9K	12.3M	1.8M	0	**0**
Acc↑ (%)	73.33	71.90	73.50	74.95	75.51	75.63	76.32	**77.50**

Table 7: Results after applying Auto Augmentation.

Teacher	WRN_40_2	WRN_40_2	VGG 13	ResNet32×4	WRN-40-2
Accuracy	75.61	75.61	74.64	79.42	75.61
Student	WRN_16_2	WRN_40_1	VGG 8	ShuffleNet-V2	ShuffleNet-V1
Accuracy	73.26	71.98	70.36	71.82	70.50
MLLD	76.63	75.35	75.18	78.44	77.44
Ours	**76.91**	**76.01**	**75.57**	**79.12**	**77.97**
Δ	+0.28	+0.66	+0.39	+0.68	+0.53

integrating projection or intermediate layers that align the teacher's feature space to the student model. With a latency of 11 ms, our method matched the best-performing models in speed and is exceptionally efficient (77.50%) without extra parameters. This combination of low latency, less computation, and high accuracy further underscores the exceptional effectiveness and efficiency of LumiNet.

Detection task: The quality of deep features is crucial for accurate object detection. One persistent challenge is effective knowledge transfer between established teacher models and student detectors (Li et al., 2017). Generally, logits cannot provide knowledge for object localization (Wang et al., 2019). Although logit-based techniques have traditionally been used for this, they often do not meet state-of-the-art standards. On **MS COCO** dataset, LumiNet delivered noticeably better results (Table 10) compared to logit-based methods, which are comparable to feature-based methods. Also, it is possible to enhance accuracy through hyperparameter tuning. Additionally, we enhance our approach by integrating a feature-based technique. The combination of these two methods yields state-of-the-art results, as detailed in the appendix.

Transfer learning task: To assess the transferability of deep features, we carry out experiments to verify the superior generalization capabilities of our algorithm LumiNet. In this context, we used the Wide Residual Network (WRN-16-2), distilled from WRN-40-2, as our principal feature extraction apparatus. Subsequently, sequential linear probing tasks were performed on the benchmark downstream dataset, notably *Tiny-ImageNet*. Our empirical results, delineated in Fig. 2(a), manifestly underscore the exemplary transferability of features cultivated through LumiNet.

Effect of Strong Augmentation: In Table 7, we report performance after using auto-augmentation by increasing the complexity of training samples (Cubuk et al., 2019). LumiNet outperforms auto augmentation-based method (Jin et al., 2023) in heterogeneous and homogeneous settings on the CIFAR-100 dataset. The results show our effectiveness in distilling knowledge from challenging samples.

Vision Transformer: To explore the capabilities of LumiNet beyond conventional ConvNet models, we performed experiments using different variants of vision transformers (ViT) in the CIFAR-100 dataset. We trained ViT with the optimal distiller obtained using ResNet-56 as a CNN teacher. Table 8 presents the results of experiments that involve both vanilla and distillation models in a variety of distillation methods.

Table 8: Top-1 mean accuracy (%) comparison on CIFAR-100

Student	Vanilla	KD	AT	SP	LG	AutoKD	Ours	Δ
DeiT-Ti	65.08	73.25	73.51	67.36	78.15	78.58	**79.05**	+5.8
PiT-Ti	73.58	75.47	76.03	74.97	78.48	78.51	**79.80**	+4.33
PVT-Ti	69.22	73.60	74.66	70.48	77.07	77.48	**78.12**	+4.52
PVTv2-B0	77.44	78.81	78.64	78.33	79.30	79.37	**79.94**	+1.13

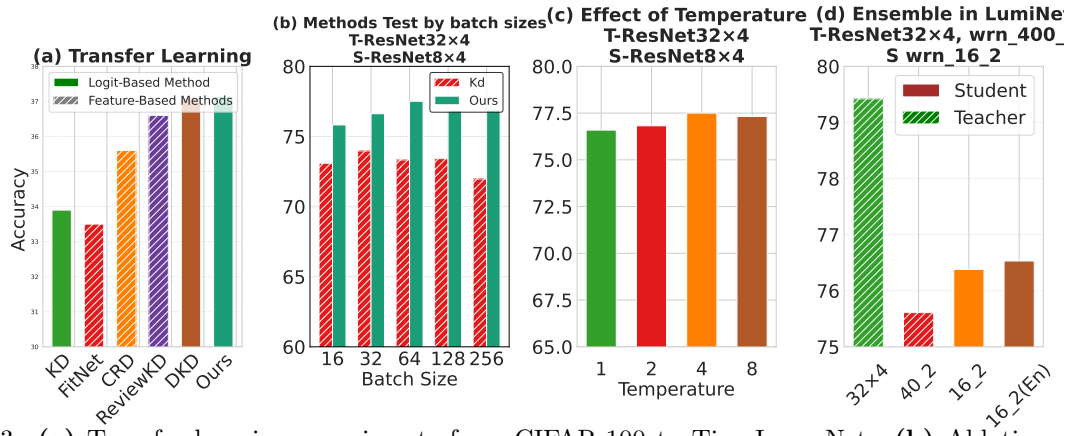

Figure 3: **(a)** Transfer learning experiments from CIFAR-100 to Tiny-ImageNet. **(b)** Ablation study on different batch sizes. **(c)** Impact of different τ values. **(d)** Performance on ensemble learning.

The results indicate a notable improvement in the performance of vision transformers with the application of LumiNet, showcasing improvements ranging from 2% to 14% compared to vanilla. In particular, LumiNet consistently outperforms other methods, demonstrating improvements of 1 to 6% compared to KD, particularly. The effectiveness of our proposed method is affirmed in various ViT architectures, highlighting its versatility. It is essential to emphasize that our approach, despite being a straightforward logit-based(soft logits) method in this context, proves to be more effective in transformer-based architectures compared to feature-based distillation methods.

4.3 Ablation study

Varying batch sizes: Fig. 3(b) showcases an ablation study that compares the performance of the LumiNet method with both a basic student model and the KD method in various batch sizes. Batch sizes range from 32 to 256. The student model, which serves as a standard baseline, demonstrates a slight decline in performance as the batch size increases. In comparison, LumiNet consistently outperforms both the student and the KD methods in all batch sizes tested, suggesting its robustness and superiority in the given context.

Varying τ: The logits within our perception framework are reconstructed with a clear statistical understanding of intra-class logits. For this, both the teacher and the student models exhibit "softened" values, achieved through normalization by variance and maintaining an intra-class mean of zero. Consequently, the dependency on temperature τ is minimal. Empirical evaluations in Fig. 3(c) suggest minimal performance fluctuations across τ (ranging between 1 and 8) yield optimal results.

Ensemble of teachers: We employ an ensemble of two teacher models: ResNet 8x4 and WRN-40-2 (labeled in the figure as "8x4" and "40-2"). This ensemble technique, which we term "Logit Averaging Ensemble," involves averaging the logits produced by the two teacher models (Sagi & Rokach, 2018). When training the student model, WRN-16-2 (labeled as "16-2" for the regular student and "16-2(en)" for the student learned by ensemble technique), we observed a notable improvement in accuracy using this ensemble-derived guidance. As shown in Fig. 3(d), when conventionally training with our LumiNet approach with only the WRN-40-2 teacher, we achieve an accuracy of 76. 38%. However, the results improve slightly to 76. 52% when training is augmented with insights from the ensemble technique. This suggests that the ensemble's aggregated information potentially enables the student model to capture more intricate patterns and nuances from the teachers.

4.4 Discussion

Achievments of LumiNet: LumiNet addresses a fundamental challenge in knowledge distillation. The inherent capacity gap between teacher and student models manifests in their logit distributions. Traditional methods often struggle when student models, with their limited capacity, attempt to match the complex,

high-variance logit distributions of teacher models. This perception-based calibration simultaneously normalizes both teacher and student logits, significantly reducing their distributional variance and eliminating teacher overconfidence. This dual calibration effectively narrows the representational gap between models, making it easier for the student to converge to optimal solutions despite its capacity constraints. The empirical evidence supports this through improved gradient flow (3.27 L2 norm compared to KD's 1.28) and higher entropy scores (1.26 versus 0.42), demonstrating that when both teacher and student operate in a more balanced, normalized logit space, the student can more effectively learn and generalize despite its architectural limitations. The experiments show that LumiNet outperforms numerous benchmark datasets, including CIFAR-100, ImageNet, and MS-COCO. We observed accuracy gains ranging from 1.5% to 4.17% over classic distillation methods, without additional parameters in training settings.

In addition, it likely solves another known problem in KD. When kD is performed per instance, the student model risks inheriting errors or biases from the teacher, a problem known as teacher-student fooling(Ojha et al., 2023). LumiNet mitigates this by incorporating relationships across all instances in a batch and recalibrating logits using batch-level statistics. With batches randomly sampled and later recalibrated the logits space by considering other samples in the batch, no single instance disproportionately influences the student, reducing the chance of transferring biases or errors. This ensures a more robust and generalized student model, resilient to dataset imperfections and teacher model flaws.

Limiation: LumiNet has some drawbacks in spite of its advantages. In complex or multi-modal tasks where intermediate feature representations are essential, it might not perform likewise. The performance of the model with small or less diverse batches may be limited by its dependence on batch-level relationships. Although LumiNet has demonstrated impressive performance in computer vision tasks, it is still unclear if it can be applied to non-visual fields like natural language processing.

Future work: Future research could examine LumiNet's approach to KD outside of computer vision, as it is thought to have significant potential in other disciplines. The perception-based logit calibration technique could be used to improve the deployment and compression of large language models in resource-constrained environments. Furthermore, LumiNet could be used for continual learning settings to investigate how the method can aid in successful knowledge acquisition while avoiding catastrophic forgetting.

5 Conclusion

We propose LumiNet, a novel knowledge distillation method, which introduces a unique representation for instances through a concept we term 'perception.'In this novel representation, we depart from the fundamental philosophy of classical KD, which centers around extracting relative information from the teacher model. Within this framework, our main focus lies on addressing overconfidence issues to achieve improved optimization. It also tackles the capacity gap issue, where the student model struggles to learn due to the high variance in the teacher model's logit distribution. In addition, we integrate statistical knowledge from other instances into an instance, resulting in a substantial improvement in accuracy compared to leading methods, which mitigates the problem of teacher-student fooling, where the student model can be misled by the teacher when it only relies on sole instance distributions. Also, LumiNet demonstrates efficiency on par with traditional KD, solidifying its suitability for industry adoption. Our comprehensive empirical experiments, spanning recognition using both convnets and vision transformers, detection, and transfer learning, consistently highlight the superior performance of LumiNet.

References

Yoshua Bengio, Aaron Courville, and Pascal Vincent. Representation learning: A review and new perspectives. *IEEE transactions on pattern analysis and machine intelligence*, 35(8):1798–1828, 2013. 2

Junyi Chai, Taeuk Jang, and Xiaoqian Wang. Fairness without demographics through knowledge distillation. *Advances in Neural Information Processing Systems*, 35:19152–19164, 2022. 4

Defang Chen, Jian-Ping Mei, Yuan Zhang, Can Wang, Zhe Wang, Yan Feng, and Chun Chen. Cross-layer distillation with semantic calibration. In *Proceedings of the AAAI Conference on Artificial Intelligence*, volume 35, pp. 7028–7036, 2021a. 2

Pengguang Chen, Shu Liu, Hengshuang Zhao, and Jiaya Jia. Distilling knowledge via knowledge review. In *Proceedings of the IEEE/CVF Conference on Computer Vision and Pattern Recognition*, pp. 5008–5017, 2021b. 4, 9, 10, 19

Jang Hyun Cho and Bharath Hariharan. On the efficacy of knowledge distillation. In *Proceedings of the IEEE/CVF international conference on computer vision*, pp. 4794–4802, 2019. 10, 19

Ekin D Cubuk, Barret Zoph, Dandelion Mane, Vijay Vasudevan, and Quoc V Le. Autoaugment: Learning augmentation strategies from data. In *Proceedings of the IEEE/CVF conference on computer vision and pattern recognition*, pp. 113–123, 2019. 11

Alexey Dosovitskiy, Lucas Beyer, Alexander Kolesnikov, Dirk Weissenborn, Xiaohua Zhai, Thomas Unterthiner, Mostafa Dehghani, Matthias Minderer, Georg Heigold, Sylvain Gelly, Jakob Uszkoreit, and Neil Houlsby. An image is worth 16x16 words: Transformers for image recognition at scale. In *International Conference on Learning Representations*, 2021. 9

Tommaso Furlanello, Zachary Lipton, Michael Tschannen, Laurent Itti, and Anima Anandkumar. Born again neural networks. In *International Conference on Machine Learning*, pp. 1607–1616. PMLR, 2018. 1

Ian J Goodfellow, Jonathon Shlens, and Christian Szegedy. Explaining and harnessing adversarial examples. In *International Conference on Learning Representations*, 2015. 1

Kaiming He, Xiangyu Zhang, Shaoqing Ren, and Jian Sun. Deep residual learning for image recognition. In *Proceedings of the IEEE conference on computer vision and pattern recognition*, pp. 770–778, 2016. 4, 9

Byeongho Heo, Jeesoo Kim, Sangdoo Yun, Hyojin Park, Nojun Kwak, and Jin Young Choi. A comprehensive overhaul of feature distillation. In *Proceedings of the IEEE/CVF International Conference on Computer Vision*, pp. 1921–1930, 2019a. 2, 4, 9

Byeongho Heo, Minsik Lee, Sangdoo Yun, and Jin Young Choi. Knowledge transfer via distillation of activation boundaries formed by hidden neurons. In *Proceedings of the AAAI Conference on Artificial Intelligence*, volume 33, pp. 3779–3787, 2019b. 4

Byeongho Heo, Sangdoo Yun, Dongyoon Han, Sanghyuk Chun, Junsuk Choe, and Seong Joon Oh. Rethinking spatial dimensions of vision transformers. In *Proceedings of the IEEE/CVF International Conference on Computer Vision*, pp. 11936–11945, 2021. 9

Geoffrey Hinton, Oriol Vinyals, and Jeff Dean. Distilling the knowledge in a neural network. *arXiv preprint arXiv:1503.02531*, 2015. 1, 4, 5, 9, 10, 18

Md Ismail Hossain, Mohammed Rakib, Sabbir Mollah, Fuad Rahman, and Nabeel Mohammed. Lila-boti: Leveraging isolated letter accumulations by ordering teacher insights for bangla handwriting recognition. In *2022 26th International Conference on Pattern Recognition (ICPR)*, pp. 1770–1776. IEEE, 2022. 4

Tao Huang, Yuan Zhang, Mingkai Zheng, Shan You, Fei Wang, Chen Qian, and Chang Xu. Knowledge diffusion for distillation. *Advances in Neural Information Processing Systems*, 36, 2024. 4

Ying Jin, Jiaqi Wang, and Dahua Lin. Multi-level logit distillation. In *Proceedings of the IEEE/CVF Conference on Computer Vision and Pattern Recognition*, pp. 24276–24285, 2023. 2, 5, 11

Sangwon Jung, Donggyu Lee, Taeeon Park, and Taesup Moon. Fair feature distillation for visual recognition. In *Proceedings of the IEEE/CVF conference on computer vision and pattern recognition*, pp. 12115–12124, 2021. 4

Taehyeon Kim, Jaehoon Oh, Nak Yil Kim, Sangwook Cho, and Se-Young Yun. Comparing kullback-leibler divergence and mean squared error loss in knowledge distillation. In Zhi-Hua Zhou (ed.), *Proceedings of the Thirtieth International Joint Conference on Artificial Intelligence, IJCAI-21*, pp. 2628–2635. International Joint Conferences on Artificial Intelligence Organization, 8 2021. doi: 10.24963/ijcai.2021/362. URL https://doi.org/10.24963/ijcai.2021/362. Main Track. 2

Yoon Kim and Alexander M Rush. Sequence-level knowledge distillation. In *Proceedings of the 2016 Conference on Empirical Methods in Natural Language Processing*, pp. 1317–1327, 2016. 4

Alex Krizhevsky, Geoffrey Hinton, et al. Learning multiple layers of features from tiny images. *Master's thesis, University of Tront*, 2009. 8

Alex Krizhevsky, Ilya Sutskever, and Geoffrey E Hinton. Imagenet classification with deep convolutional neural networks. *Advances in neural information processing systems*, 25, 2012. 4

Gang Li, Xiang Li, Yujie Wang, Shanshan Zhang, Yichao Wu, and Ding Liang. Knowledge distillation for object detection via rank mimicking and prediction-guided feature imitation. In *Proceedings of the AAAI Conference on Artificial Intelligence*, volume 36, pp. 1306–1313, 2022a. 4

Kehan Li, Runyi Yu, Zhennan Wang, Li Yuan, Guoli Song, and Jie Chen. Locality guidance for improving vision transformers on tiny datasets. In *European Conference on Computer Vision*, pp. 110–127. Springer, 2022b. 10, 19

Quanquan Li, Shengying Jin, and Junjie Yan. Mimicking very efficient network for object detection. In *Proceedings of the ieee conference on computer vision and pattern recognition*, pp. 6356–6364, 2017. 11

Tsung-Yi Lin, Michael Maire, Serge Belongie, James Hays, Pietro Perona, Deva Ramanan, Piotr Dollár, and C Lawrence Zitnick. Microsoft coco: Common objects in context. In *Computer Vision–ECCV 2014: 13th European Conference, Zurich, Switzerland, September 6-12, 2014, Proceedings, Part V 13*, pp. 740–755. Springer, 2014. 9

Tsung-Yi Lin, Piotr Dollár, Ross Girshick, Kaiming He, Bharath Hariharan, and Serge Belongie. Feature pyramid networks for object detection. In *Proceedings of the IEEE conference on computer vision and pattern recognition*, pp. 2117–2125, 2017. 10, 19

Bernadette Lindorfer. Personality theory in gestalt theoretical psychotherapy: Kurt lewin?s field theory and his theory of systems in tension revisited. *Gestalt Theory*, 43(1):29–46, 2021. doi: 10.2478/gth-2021-0002. 3

Dongyang Liu, Meina Kan, Shiguang Shan, and Xilin CHEN. Function-consistent feature distillation. In *The Eleventh International Conference on Learning Representations*, 2023a. 9

Xiaolong Liu, LUKING LI, Chao Li, and Anbang Yao. NORM: Knowledge distillation via n-to-one representation matching. In *The Eleventh International Conference on Learning Representations*, 2023b. URL https://openreview.net/forum?id=CRNwGauQpb6. 5

Yifan Liu, Ke Chen, Chris Liu, Zengchang Qin, Zhenbo Luo, and Jingdong Wang. Structured knowledge distillation for semantic segmentation. In *Proceedings of the IEEE/CVF conference on computer vision and pattern recognition*, pp. 2604–2613, 2019. 4

Ningning Ma, Xiangyu Zhang, Hai-Tao Zheng, and Jian Sun. Shufflenet v2: Practical guidelines for efficient cnn architecture design. In *Proceedings of the European conference on computer vision (ECCV)*, pp. 116–131, 2018. 9

Seyed Iman Mirzadeh, Mehrdad Farajtabar, Ang Li, Nir Levine, Akihiro Matsukawa, and Hassan Ghasemzadeh. Improved knowledge distillation via teacher assistant. In *Proceedings of the AAAI conference on artificial intelligence*, volume 34, pp. 5191–5198, 2020. 1, 4, 5, 9, 10

Utkarsh Ojha, Yuheng Li, Anirudh Sundara Rajan, Yingyu Liang, and Yong Jae Lee. What knowledge gets distilled in knowledge distillation? *Advances in Neural Information Processing Systems*, 36:11037–11048, 2023. 3, 13

Wonpyo Park, Dongju Kim, Yan Lu, and Minsu Cho. Relational knowledge distillation. In *Proceedings of the IEEE/CVF conference on computer vision and pattern recognition*, pp. 3967–3976, 2019. 4, 9, 10

Dian Qin, Jia-Jun Bu, Zhe Liu, Xin Shen, Sheng Zhou, Jing-Jun Gu, Zhi-Hua Wang, Lei Wu, and Hui-Fen Dai. Efficient medical image segmentation based on knowledge distillation. *IEEE Transactions on Medical Imaging*, 40(12):3820–3831, 2021. 4

Kazi Rafat, Sadia Islam, Abdullah Al Mahfug, Md. Ismail Hossain, Fuad Rahman, Sifat Momen, Shafin Rahman, and Nabeel Mohammed. Mitigating carbon footprint for knowledge distillation based deep learning model compression. *PLOS ONE*, 18(5):1–22, 05 2023. 5

Adriana Romero, Nicolas Ballas, Samira Ebrahimi Kahou, Antoine Chassang, Carlo Gatta, and Yoshua Bengio. Fitnets: Hints for thin deep nets. *arXiv preprint arXiv:1412.6550*, 2014. 1, 2, 4, 5, 9, 10

Olga Russakovsky, Jia Deng, Hao Su, Jonathan Krause, Sanjeev Satheesh, Sean Ma, Zhiheng Huang, Andrej Karpathy, Aditya Khosla, Michael Bernstein, et al. Imagenet large scale visual recognition challenge. *International journal of computer vision*, 115:211–252, 2015. 8

Omer Sagi and Lior Rokach. Ensemble learning: A survey. *Wiley Interdisciplinary Reviews: Data Mining and Knowledge Discovery*, 8(4):e1249, 2018. 12

Mark Sandler, Andrew Howard, Menglong Zhu, Andrey Zhmoginov, and Liang-Chieh Chen. Mobilenetv2: Inverted residuals and linear bottlenecks. In *Proceedings of the IEEE conference on computer vision and pattern recognition*, pp. 4510–4520, 2018. 9

Karen Simonyan and Andrew Zisserman. Very deep convolutional networks for large-scale image recognition. *arXiv preprint arXiv:1409.1556*, 2014. 4, 9

Yaoye Song, Peng Zhang, Wei Huang, Yufei Zha, Tao You, and Yanning Zhang. Closed-loop unified knowledge distillation for dense object detection. *Pattern Recognition*, 149:110235, 2024. 4

Yonglong Tian, Dilip Krishnan, and Phillip Isola. Contrastive representation distillation. In *International Conference on Learning Representations*, 2020. 1, 4, 9, 10, 19

Hugo Touvron, Matthieu Cord, Matthijs Douze, Francisco Massa, Alexandre Sablayrolles, and Hervé Jégou. Training data-efficient image transformers & distillation through attention. In *International conference on machine learning*, pp. 10347–10357. PMLR, 2021. 9

Frederick Tung and Greg Mori. Similarity-preserving knowledge distillation. In *Proceedings of the IEEE/CVF international conference on computer vision*, pp. 1365–1374, 2019. 1, 4

Ashish Vaswani, Noam Shazeer, Niki Parmar, Jakob Uszkoreit, Llion Jones, Aidan N Gomez, Łukasz Kaiser, and Illia Polosukhin. Attention is all you need. *Advances in neural information processing systems*, 30, 2017. 1

Lin Wang and Kuk-Jin Yoon. Knowledge distillation and student-teacher learning for visual intelligence: A review and new outlooks. *IEEE transactions on pattern analysis and machine intelligence*, 44(6):3048–3068, 2021. 2

Tao Wang, Li Yuan, Xiaopeng Zhang, and Jiashi Feng. Distilling object detectors with fine-grained feature imitation. In *Proceedings of the IEEE/CVF Conference on Computer Vision and Pattern Recognition*, pp. 4933–4942, 2019. 11

Wenhai Wang, Enze Xie, Xiang Li, Deng-Ping Fan, Kaitao Song, Ding Liang, Tong Lu, Ping Luo, and Ling Shao. Pyramid vision transformer: A versatile backbone for dense prediction without convolutions. In *Proceedings of the IEEE/CVF international conference on computer vision*, pp. 568–578, 2021. 9

Wenhai Wang, Enze Xie, Xiang Li, Deng-Ping Fan, Kaitao Song, Ding Liang, Tong Lu, Ping Luo, and Ling Shao. Pvt v2: Improved baselines with pyramid vision transformer. *Computational Visual Media*, 8(3): 415–424, 2022. 9

Peter West, Chandra Bhagavatula, Jack Hessel, Jena Hwang, Liwei Jiang, Ronan Le Bras, Ximing Lu, Sean Welleck, and Yejin Choi. Symbolic knowledge distillation: from general language models to commonsense models. In Marine Carpuat, Marie-Catherine de Marneffe, and Ivan Vladimir Meza Ruiz (eds.), *Proceedings of the 2022 Conference of the North American Chapter of the Association for Computational Linguistics: Human Language Technologies*, pp. 4602–4625, Seattle, United States, July 2022. Association for Computational Linguistics. doi: 10.18653/v1/2022.naacl-main.341. URL https://aclanthology.org/2022.naacl-main.341. 4

Yufei Xu, Jing Zhang, Qiming Zhang, and Dacheng Tao. Vitpose: Simple vision transformer baselines for human pose estimation. *Advances in Neural Information Processing Systems*, 35:38571–38584, 2022. 4

Chenglin Yang, Lingxi Xie, Siyuan Qiao, and Alan Loddon Yuille. Training deep neural networks in generations: A more tolerant teacher educates better students. In *AAAI Conference on Artificial Intelligence*, 2018. 1

Jihan Yang, Shaoshuai Shi, Runyu Ding, Zhe Wang, and Xiaojuan Qi. Towards efficient 3d object detection with knowledge distillation. *Advances in Neural Information Processing Systems*, 35:21300–21313, 2022. 4

Bayya Yegnanarayana. *Artificial neural networks*. PHI Learning Pvt. Ltd., 2009. 5

Junho Yim, Donggyu Joo, Jihoon Bae, and Junmo Kim. A gift from knowledge distillation: Fast optimization, network minimization and transfer learning. In *Proceedings of the IEEE conference on computer vision and pattern recognition*, pp. 4133–4141, 2017. 1

Sergey Zagoruyko and Nikos Komodakis. Paying more attention to attention: Improving the performance of convolutional neural networks via attention transfer. In *International Conference on Learning Representations*, 2017. 4

Bowen Zhang, Xu Huang, Zhichao Huang, Hu Huang, Baoquan Zhang, Xianghua Fu, and Liwen Jing. Sentiment interpretable logic tensor network for aspect-term sentiment analysis. In *Proceedings of the 29th International Conference on Computational Linguistics*, pp. 6705–6714, 2022. 4, 9

Ying Zhang, Tao Xiang, Timothy M Hospedales, and Huchuan Lu. Deep mutual learning. In *Proceedings of the IEEE conference on computer vision and pattern recognition*, pp. 4320–4328, 2018. 1, 4, 5, 9, 10

Borui Zhao, Quan Cui, Renjie Song, Yiyu Qiu, and Jiajun Liang. Decoupled knowledge distillation. In *Proceedings of the IEEE/CVF Conference on computer vision and pattern recognition*, pp. 11953–11962, 2022. 1, 2, 4, 5, 9, 10, 18

Zhaohui Zheng, Rongguang Ye, Qibin Hou, Dongwei Ren, Ping Wang, Wangmeng Zuo, and Ming-Ming Cheng. Localization distillation for object detection. *IEEE Transactions on Pattern Analysis and Machine Intelligence*, 2023. 4

Helong Zhou, Liangchen Song, Jiajie Chen, Ye Zhou, Guoli Wang, Junsong Yuan, and Qian Zhang. Rethinking soft labels for knowledge distillation: A bias–variance tradeoff perspective. In *International Conference on Learning Representations*, 2021. 4

Dongyao Zhu, Bowen Lei, Jie Zhang, Yanbo Fang, Yiqun Xie, Ruqi Zhang, and Dongkuan Xu. Rethinking data distillation: Do not overlook calibration. In *Proceedings of the IEEE/CVF International Conference on Computer Vision*, pp. 4935–4945, 2023. 1

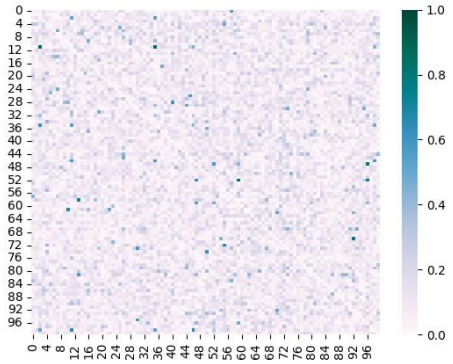

Figure 4: Comparing teacher-student prediction similarity in DKD method.

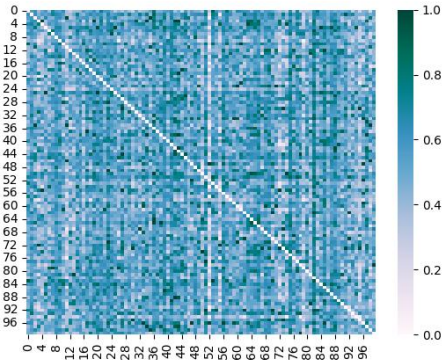

Figure 5: Comparing Teacher-Student Predictions Similarity in Our Method

A Appendix

A.1 Alternative Perspective on Traditional Knowledge Distillation Method.

The primary goal of traditional knowledge distillation is to replicate the raw logits of the teacher, as illustrated in Fig 4. This figure demonstrates that the predictions closely resemble the teacher's logits.In this method, we often face overconfidence issues, resulting in inferior performance compared to feature-based KD. Moreover, despite our aim to mimic the logits of the teacher, a substantial gap persists between teachers and students. However, in our approach, *LumiNet*, depicted in Figure 5, the prediction similarity to the teacher's logits is significantly lower compared to DKD. Yet, as detailed in the main paper, *LumiNet* achieves better performance scores than DKDZhao et al. (2022) also, the gap between teacher and student is minimized. Importantly, teacher and student predictions are independent, diverging from similar logits. This indicates that, in logit-based distillation, we can achieve superior performance without directly mimicking the raw logits. Also, within the parameters, the student models are capable of independently learning features through their innate pattern recognition abilities without being explicitly guided to mimic the pattern learning process of the teacher model. Consequently, this empowers the student model to create new representations and inter-class relationships for instances, a capability that traditional knowledge distillation methods lack.

A.2 Implementation detail

For a fair comparison, we maintain a similar setup to previous methodsHinton et al. (2015); Zhao et al. (2022). In traditional KDHinton et al. (2015), both Cross-Entropy loss and Kullback-Leibler (KL) Divergence loss are employed. Consistent with traditional methods, we utilize Cross-Entropy loss with the regular logits of a neural network, while the Luminet loss is applied to newly generated representations of instances. Further details of the Luminet loss are provided in the main paper. In this scenario, the hyperparameter α is set such that $\alpha > t^2$, where α represents a constant associated with the Luminet loss when combined with Cross-Entropy loss and t represents temperature. Specific implementation details for each task are outlined below.

Image Recognition: For training a student model on the CIFAR-100 dataset, we use a batch size of 64 and train for a total of 240 epochs. The initial learning rate (LR) is set to 0.05, with learning rate decay applied at epochs 150, 180, and 210, where the LR is reduced by a factor of 0.1 each time. We employ a weight decay of 0.0005 and a momentum of 0.9 in our stochastic gradient descent (SGD) optimizer.

When training on the ImageNet dataset, we use a batch size of 512 and train for a total of 100 epochs. The initial LR is set to 0.2, with learning rate decay scheduled at epochs 30, 60, and 90, where the LR is decreased by a factor of 0.1 each time. We apply a weight decay of 0.0001 and utilize a momentum of 0.9 in the SGD optimizer.

Table 9: Performance of our method with the incorporation of ReviewKD Loss on CIFAR-100 dataset

Teacher/Student Architecture	**ReviewKD**	**Ours**	**Ours***
WRN-40-2 → ShuffleNet-V1	77.14	76.95	**77.29**
ResNet32×4 → ShuffleNet-V2	77.78	77.55	**77.93**

Table 10: Detection results on MS-COCO using Faster-RCNN-FPN Lin et al. (2017) backbone with incorporating ReviewKD.

			Feature-Based Methods			Logit-Based Methods				
ResNet101 (Teacher) and ResNet18 (Student)										
	Teacher	Student	FitNet	FGFI	ReviewKD	KD	TAKD	DKD	Ours	Ours*
AP	42.04	33.26	34.13	35.44	36.75	33.97	34.59	35.05	35.34	**36.89**
AP_{50}	62.48	53.61	54.16	55.51	56.72	54.66	55.35	56.60	56.82	**57.05**
AP_{75}	45.88	35.26	36.71	38.17	34.00	36.62	37.12	37.54	37.56	**39.59**
ResNet50 (Teacher) and MobileNet-V2 (Student)										
AP	40.22	29.47	30.20	31.16	33.71	30.13	31.26	32.34	32.38	**34.18**
AP_{50}	61.02	48.87	49.80	50.68	53.15	50.28	51.03	53.77	53.84	**53.95**
AP_{75}	45.88	30.90	31.69	32.92	36.13	31.35	33.46	34.01	33.57	**36.44**

Object Detection: For training object detection student models on the MS-COCO 2017 dataset, we use an image per batch of 8. The base learning rate is set to 0.01, and the maximum number of iterations is set to 180,000. Learning rate decay is applied at specific steps during training, with decay steps set at 120,000 and 160,000 iterations.

Vision Transformer We adopt the settings described in reference Li et al. (2022b) for training the student model of vision transformer variants. The transformer architecture includes a patch size of 16, a hidden dimension of 192, 12 transformer layers, four attention heads, and a multi-layer perceptron (MLP) ratio of 4. We set the dropout rate to 0.0, the drop path rate to 0.1, and the attention dropout rate to 0.0. For optimization, we use the AdamW optimizer with a base learning rate of 5.0×10^{-4} and a minimum learning rate of 5.0×10^{-6}. The learning rate policy is cosine annealing (cos) with a maximum of 300 epochs. We apply a weight decay of 0.05, a warm-up factor of 0.001, and warm-up epochs of 20.

A.3 Incorporating with feature-based distillation

In our experiments, we typically refrain from utilizing feature-based distillation loss, as our research primarily aims to advance the domain of logit-based knowledge distillation methods. However, in certain architectures, and to explore its compatibility with existing feature-based KD methods, we incorporated the feature-based loss (ReviewKD Chen et al. (2021b)) alongside our *LumiNet* loss.

This combination resulted in significant performance improvements, as demonstrated in Table 9 for the image recognition task and Table 10 for the object detection task. In the tables, the asterisk (*) denotes the utilization of the combined loss function. Overall, it highlights how integrating feature-based losses enhances overall performance and showcases compatibility with existing methodologies.

Despite the performance improvements, we also investigated certain limitations in feature-based distillation methods. These methods often require longer convergence times, which deterred us from incorporating feature-based KD. For instance, ReviewKD Chen et al. (2021b), despite its comprehensive approach, requires significant training time due to its multi-level distillation process and complex components like the Attention-Based Fusion module. OFD Cho & Hariharan (2019), while focusing on multi-layer distillation, demands extra convolutions for feature alignment, increasing computational needs. Similarly, CRD Tian et al. (2020) employs a contrastive loss that requires a large memory bank, adding to computational costs.

In summary, while incorporating feature-based logits into our knowledge distillation method yields better results, it also introduces significant drawbacks in terms of privacy, computational requirements, and training

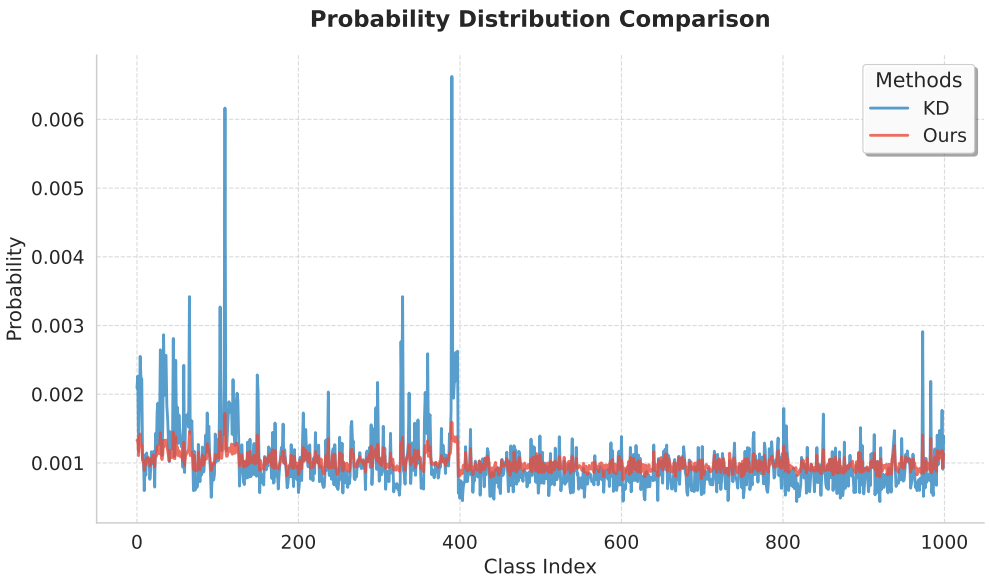

Figure 6: Comparison of probability distributions between traditional KD and our proposed method on ImageNet using ResNet18. The blue line represents temperature-scaled KD (T=4), showing multiple high-confidence regions and significant disparities between target and non-target classes. The red line shows our method's distribution, which effectively reduces both the class dwarfing effect (lower peaks) and multi-modal nature of the distribution, resulting in more manageable class relationships for the student model to learn. This visualization demonstrates how our approach simplifies the dark knowledge transfer while maintaining informative class relationships across the 1000 ImageNet classes.

time. Hence, we advocate for logit-based knowledge distillation as a more resource-efficient and versatile alternative for various applications.

A.4 Logit Complexity Analysis

Neural knowledge distillation faces inherent challenges due to the architectural capacity gap between teacher and student models, where students with fewer parameters struggle to directly mimic the complex distributions generated by larger teachers. Two critical issues arise in traditional KD. First, there is a significant disparity between the probabilities of target and non-target classes. The teacher model tends to produce overly confident predictions for the target classes, which creates a considerable learning burden for the student model, as discussed in section X of the paper. Second, this challenge intensifies with an increasing number of classes, manifesting as multiple high-probability regions (multi-mode) across the class space. These issues become particularly pronounced in large language models, where the vocabulary size far exceeds typical image classification tasks [cite], resulting in substantially more complex probability distributions for the student to learn. Our perception-based approach effectively addresses these limitations by significantly reducing the class dwarfing effect and diminishing the multi-mode peaks, as demonstrated in Figure 6. Using ResNet18 on ImageNet (1000 classes), we observe that our method produces more balanced probability distributions compared to temperature-scaled KD (T=4), making the dark knowledge transfer more tractable for the student model while preserving essential class relationships.

A.5 LumiNet in Large-Language Model

KD in Large Language Models (LLMs) presents unique challenges compared to its application in computer vision tasks. In vision models, the logit distribution usually displays a single-mode pattern, making it relatively easy for student models to replicate the teacher's probability distribution. However, LLMs operate with vocabulary spaces that span thousands to millions of tokens, resulting in complex 'multi-mode' dis-

Table 11: Evaluation results. We report the average R-L scores across 5 random seeds. The best scores of each model size are boldfaced, and the scores where the student model outperforms the teacher are marked with *.

Model	#Params	Method	Dolly	SelfInst	Vicuna
Teacher	1.5B	-	27.6	14.3	16.3
GPT-2	120M	SFT w/o KD	23.3	10.0	14.7
		KD	22.8	10.8	13.4
		SeqKD	22.7	10.1	14.3
		Ours	**23.8**$_{(0.37)}$	**11.4**$_{(0.42)}$	**14.9**$_{(0.10)}$
	340M	SFT w/o KD	25.5	13.0	16.0
		KD	25.0	12.0	15.4
		SeqKD	25.3	12.6	16.9*
		Ours	**27.8***$_{(0.47)}$	**13.8**$_{(0.48)}$	**17.1***$_{(0.16)}$
	760M	SFT w/o KD	25.4	12.4	16.1
		KD	25.9	13.4	16.9*
		SeqKD	25.6	14.0	15.9
		Ours	**28.6***$_{(0.49)}$	**14.7***$_{(0.19)}$	**17.5***$_{(0.10)}$

tributions for a sample. This fundamental difference makes traditional KD approaches less effective for LLMs.

We used the dataset split within this space for our experiment[2]. We have used 13.5k samples from the Dolly dataset for fine-tuning, while 500 samples were reserved for testing. Additionally, 80 and 240 samples were used from Vicuna and SelfInst, respectively for evaluation. We have adapted our method to make it suitable for LLMs. Our experimental results, as shown in Table 11, demonstrate that our method consistently outperforms existing KD approaches across different model sizes. For instance, with GPT-2 340M as the student model, our method achieves 27.8, 13.8, and 17.1 R-L scores on Dolly, SelfInst, and Vicuna test sets, respectively, surpassing both conventional KD (25.0, 12.0, 15.4) and Sequential KD. Notably, in several cases, our student models even outperform the 1.5B teacher model.

For our experimental setup, we used a 1.5B parameter model as the teacher and tested student models of varying sizes (120M, 340M, and 760M parameters) based on the GPT-2 architecture. The training was conducted with a batch size of 2. We implemented sequence-level tokenization and used the AdamW optimizer with a learning rate of 5e-5. The training was performed on a single 4090 GPU.

A.6 Confirmation Bias Analysis

To empirically validate our hypothesis about confirmation bias in knowledge distillation, we analyze the error rates across different classes, particularly focusing on the classes where the teacher model performs poorly. Table 12 presents the error rates for the top 10 most challenging classes for the teacher model (ResNet32x4), comparing them with both traditional KD and our proposed method using ResNet8x4 as the student architecture. The results provide strong evidence of confirmation bias in traditional KD. For most difficult classes where the teacher exhibits high error rates (ranging from 34% to 45%), the KD student model not only inherits these mistakes but often amplifies them. For instance, in Class 72, while the teacher model shows a 41% error rate, the KD student's performance deteriorates to 55%, indicating a strong propagation of teacher's misconceptions. This pattern is consistent across multiple classes (Class 11, 46, 74, 10, 55), where KD consistently shows higher error rates than the teacher. In contrast, our proposed method demonstrates remarkable resilience to confirmation bias. In 6 out of 10 challenging classes (marked with asterisks), our approach achieves lower error rates than the teacher model, effectively breaking the cycle of error propagation. Most notably, in Class 46 and Class 74, our method reduces the error rates from 42% and 40% to 38% and 37% respectively, showing that the student can actually outperform the teacher in

[2] https://huggingface.co/MiniLLM

Table 12: Error Rates by Class and Method for the Top 10 Most Inaccurate Classes of the Teacher Models. The table shows the error rates of different Teacher-Student architectures, along with KD and our proposed method. An asterisk (*) indicates an error rate lower than the Teacher model's error rate. Our proposed method consistently outperforms KD across different architectures.

Teacher (ResNet32x4) - Student(ResNet8x4)										
Method	**C35 (Bee)**	**C11 (Poppies)**	**C46 (Castle)**	**C72 (Girl)**	**C74 (Woman)**	**C52 (Mountain)**	**C64 (Skunk)**	**C10 (Orchids)**	**C55 (Camel)**	**C50 (Cloud)**
Teacher	45.0	43.0	42.0	41.0	40.0	39.0	38.0	37.0	36.0	34.0
KD	**43.0***	49.0	47.0	55.0	47.0	40.0	43.0	42.0	49.0	38.0
Ours	46.0	**47.0**	**38.0***	**52.0**	**37.0***	**37.0***	**38.0***	**36.0***	**44.0**	**38.0**
Teacher (WideResNet-40-2) - Student(WideResNet-40-1)										
Method	**C72 (Girl)**	**C35 (Bee)**	**C55 (Camel)**	**C10 (Orchids)**	**C50 (Cloud)**	**C46 (Castle)**	**C64 (Skunk)**	**C67 (Snail)**	**C11 (Poppies)**	**C74 (Woman)**
Teacher	51.0	50.0	48.0	47.0	46.0	45.0	44.0	44.0	43.0	43.0
KD	52.0	55.0	48.0	**42.0***	48.0	39.0*	44.0	47.0	52.0	47.0
Ours	53.0	**54.0**	**45.0***	45.0	**46.0***	**31.0***	**41.0***	**42.0***	**44.0**	**45.0**
Teacher (VGG13) - Student(VGG8)										
Method	**C35 (Bee)**	**C72 (Girl)**	**C55 (Camel)**	**C44 (Wolf)**	**C46 (Castle)**	**C10 (Orchids)**	**C25 (Clock)**	**C11 (Poppies)**	**C74 (Woman)**	**C64 (Skunk)**
Teacher	54.0	53.0	50.0	48.0	47.0	46.0	46.0	45.0	45.0	43.0
KD	53.0*	54.0	57.0	54.0	46.0	53.0	56.0	53.0	46.0	50.0
Ours	**53.0***	**49.0***	**45.0***	**51.0**	**44.0***	**41.0***	**33.0***	**45.0***	**45.0***	**47.0**

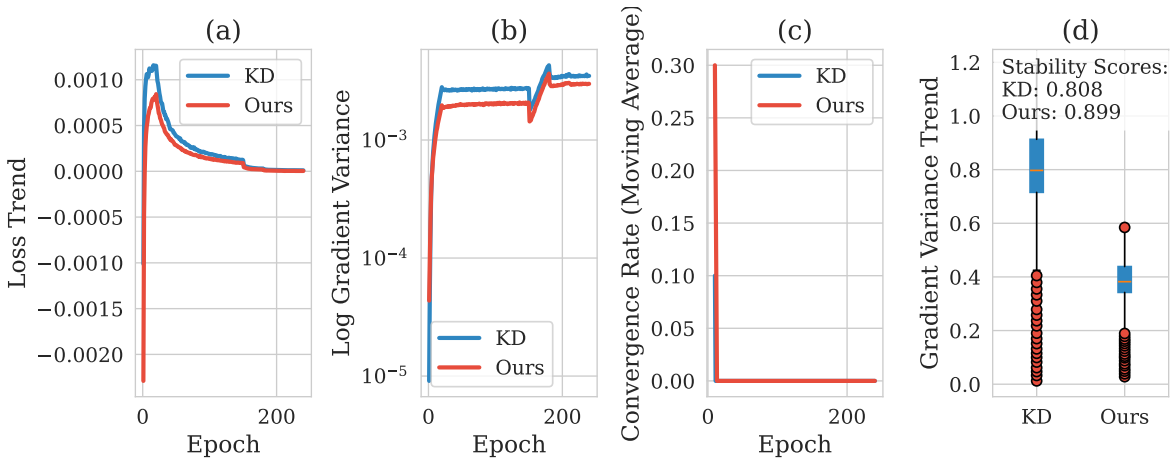

Figure 7: Comparison of various metrics between the proposed method and standard KD: (a) Loss Convergence Trend over epochs, showing the progression of training loss; (b) Gradient Variance Evaluation on a logarithmic scale, highlighting the stability of gradient updates; (c) Convergence Rate Analysis using a moving average, illustrating the rate of model convergence; (d) Gradient Stability Distribution represented by a boxplot, summarizing the distribution of gradient variance trends.

challenging cases. Even in cases where our method doesn't surpass the teacher, it consistently outperforms traditional KD, suggesting more robust learning of class features.

A.7 Convergence Analysis

In this section, we present a thorough analysis of our method's convergence properties and training stability. To establish the effectiveness of our approach, we first provide theoretical foundations for gradient stability, followed by comprehensive empirical validation through experiments.

Theoretical Analysis We show a theoretical framework demonstrating why LumiNet achieves superior stability and convergence compared to traditional KD. Consider the gradient (g_t) update at iteration t:

$$g_t = \nabla L_{CE}(\theta_t) + \lambda \nabla L_{LumiNet}(\theta_t) \tag{7}$$

Unlike traditional KD, which directly matches logit distributions and can result in conflicting gradients, LumiNet uses a perception loss that guarantees consistent gradient directions. This can be clarified through the following properties:

Property 1 (Gradient Consistency): In LumiNet, the alignment between ∇L_{CE} and $\nabla L_{LumiNet}$ is maintained through perceptual matching. This leads to:

$$\angle(\nabla L_{CE}, \nabla L_{LumiNet}) < \angle(\nabla L_{CE}, \nabla L_{KD}) \tag{8}$$

where $\angle$ denotes the angle between gradients. This smaller angle ensures more consistent optimization steps compared to KD.

Property 2 (Bounded Update Variance): The variance of gradient ($Var(g_t)$)updates in LumiNet is inherently bounded:

$$Var(g_t)LumiNet < Var(g_t)KD \tag{9}$$

This bound emerges from the perceptual alignment mechanism, which prevents the large gradient fluctuations commonly observed in KD.

Empirical Validation To validate our theoretical analysis, we implemented a comprehensive framework for measuring convergence behavior and training stability. Our framework tracks the temporal evolution of loss values, measures gradient variance across network layers, and evaluates parameter convergence rates throughout the training process. We conducted extensive experiments using the VGG8 architecture on CIFAR-100, comparing our method against traditional knowledge distillation.

Figure 7 presents the key findings of our analysis. Our method demonstrates superior stability characteristics with a stability score of 0.899 compared to KD's 0.808 (Figure 7d). The log gradient variance analysis reveals that our approach maintains consistently lower variance (10^{-4}) compared to standard KD (10^{-3}), indicating more stable parameter updates throughout training (Figure 7b). This empirical observation aligns with our theoretical bound on gradient variance.

The convergence rate analysis, depicted in Figure 7c, shows that our method achieves higher moving average convergence rates, particularly during the crucial early stages of training. Furthermore, the loss trend analysis (Figure 7a) demonstrates more stable loss reduction patterns with notably fewer fluctuations compared to standard KD, suggesting more reliable optimization behavior. The consistently lower gradient variance throughout training empirically validates our theoretical bound on $Var(g_t)$, while the more stable loss trajectory provides strong evidence for reliable optimization behavior.

Our method maintains consistent training dynamics even in later epochs, as evidenced by the stability scores and gradient variance trends. This addresses concerns regarding long-term training stability and shows that our approach converges more reliably than standard KD, while also maintaining stable training dynamics throughout the optimization process. The combination of our theoretical bounds on gradient variance and comprehensive empirical validation provides strong evidence for both the stability and effectiveness of our proposed method. The results of our analysis collectively demonstrate that our approach successfully addresses the fundamental challenges of training stability in knowledge distillation while achieving superior convergence properties.